An analytical model for the monitoring of pore water pressure inside embankment dams

X. Guo[a], J. Baroth[a], D. Dias[a,*], A. Simon[b]

[a] *Univ. Grenoble Alpes, CNRS, Grenoble INP[1], 3SR, F-38000 Grenoble, France*
[b] *EDF-DTG, 21 avenue de l'Europe, BP 41, 38000 Grenoble, France*

ABSTRACT

The hydraulic behaviour of embankment dams is influenced by many factors, such as hydrostatic loads and settlement. Particularly, the delayed response due to the diffusion phenomena plays a crucial role in the interpretation of the monitoring data gathered in embankment dams. The paper describes a statistical analysis model named EFR (EFfet Retard - Delayed effect), based on the HST (Hydrostatic-Season-Time) model, for the monitoring of pore water pressure inside embankment dams. The model allows separating the influence of the most important factors and takes into account the delayed hydrostatic effect. The use of this model leads to a better estimation of the irreversible trend and enables an earlier detection of abnormal pore water pressures. An application of this model to a French embankment dam is provided in the second part of the paper. Based on this application, the influence of different diffusion models, calculation methods for the equivalent reservoir water levels and the irreversible term versions on the EFR analysis results are discussed.

1. Introduction

According to the ICOLD (International Commission on Large Dams), the majority of failed dams either did not have any monitoring system or had a system that was out of order [1]. This finding therefore demonstrates the importance of inspection and an appropriate monitoring system for regular observation of dam performance. The objective of dam monitoring, which plays a significant role in the concept of dam safety, is to provide data in order to evaluate dam performances throughout its whole life cycle. The typical safety control variables could be classified into 3 categories: mechanical effects (deformation, displacement), hydraulic effects (seepage flow rate and pore water pressure) and environmental effects (reservoir water levels, precipitation and temperature) [2]. Such variables are quantified by means of monitoring instruments installed in dams.

Once the monitoring data is collected, it is necessary to analyze it inside and in the vicinity of the dam for the purpose of determining and understanding the dam's behaviour. Changes in the behaviour of dams in response to thermal or seasonal effects and to variations in the reservoir water level are mostly reversible. By separating the hydrostatic effect induced by the impounding variations and the thermal effects induced by the temperature variation, some aspects can be better understood. It should be noted that the thermal effects are negligible for

embankment dams, and thus can be neglected for analyzing the measurements collected in such dams. Multiple correlation methods are used to draw up models for the following-up and surveillance of monitoring measurements. Over the last fifty years, the increase of knowledge in the field of data analysis has led to the development of analytical methods which can exploit these databases, yielding excellent results [3]. The first physical-statistical model which statistically determines the effects of hydrostatic and thermal loads was formulated in 1967 [4,5]. This HST model accounts for mechanical behaviour, by using a statistical regression technique to find out correlations between causes and quantified effects. It is based on a mean seasonal thermal reference curve for the phenomena observed on dams and it enables one-year periodic variations to be identified according to the reservoir level and time. After many years using this model, its limitation was revealed by the phenomena which are sensitive to variations of temperature because it cannot take real temperature into account. In 2004, a new model named HST-T (-T for thermal) [6] was developed after the heatwave of 2003 to better consider the influences of harsh thermal conditions.

Concerning embankment dams, the monitoring of pore water pressure is crucial because it is the main indicator of internal erosion and seepage problems and has a significant role in the stability of geotechnical works [7–9]. Pagano [10] focused on these pore water

---

pressure measurements at different stages of the dam lifetime. The authors collected measurements, particularly during the consolidation process within the dam, in order to detect the effectiveness of measurements, in revealing watertightness problems. These problems are influenced by various external factors due to the fact that the effects of variations in reservoir water levels are not instantaneous since the flow inside the dams are delayed by the low hydraulic conductivity of the materials constituting the embankment. Bonelli and Royet [11] described a model, using a linear dynamic system, to perform delay analysis on pore water pressure measurements. The authors assumed that the delayed effects depend on the convolution of numerical integral of the impulse response and the loadings. However, only the non-ageing factors are modelled in the model. The irreversible trend of measurements therefore cannot be quantified. Lombardi et al. [12] suggested an equivalent formulation of delay analysis to [11], but for thermal response in concrete dams. For more information about the delayed effect analysis of dam behaviour, readers are referred to Salazar et al. [13], in which a review of statistical models for the prediction of dam behaviour is presented.

In order to tackle the problems mentioned above, the EFR model was developed for the analysis of pore water pressure measurements in embankment dams [14]. It allows taking into account delayed hydrostatic effects and obtaining the pore water pressure under identical loading conditions by identifying and separating the influence of the most important factors (ageing and non-ageing factors). The model is able to quantify the delayed hydrostatic effects and leads to a better estimation of the irreversible trend induced by sensors ageing, foundation settlements, soil consolidation and engineering works, etc. Abnormal pore water pressures evolution can be earlier detected with the model, especially in the case of low hydraulic conductivity and for the sensors located far from hydrostatic loads.

The article is organized into two parts. The first part consists in presenting the EFR model in detail, including the principle and calculation of "equivalent reservoir water level" (ERWL). The second part provides an application of the model to a French embankment dam. The underlying diffusion model, the numerical computation method for the ERWL and the irreversible term versions are discussed in this part.

2. Description of EFR model

The EFR model is an extension of the conventional HST model. It is designed for the monitoring of pore water pressure measurements in embankment dams and is able to account for delayed hydrostatic effects. For this reason, a general description of the HST model is provided at first in the section. It is followed by the development of the EFR model.

2.1. General description of the HST model

The HST model was initially proposed by Willm and Beaujoint [5] for the monitoring of global displacements in concrete dams. The model has been widely used for analyzing monitoring data of dams and has been turned out to be a powerful tool for data analysis in dams [15].

The model is based on the assumption that the displacements are mainly explained by three factors: a reversible effect of hydrostatic loads, a reversible seasonal thermal influence and an irreversible term due to the evolution response of dams over time. It consists in a multiple linear regression function Y given in Eq. (1) which is the sum of an average value a_0, different functions modelling independently the three specific factors ($f_{hydro}, f_{ther}, f_{irre}$) and ϵ a residual error [16].

$$Y = a_0 + f_{hydro} + f_{ther} + f_{irre} + \epsilon \tag{1}$$

The function f_{hydro} is usually a polynomial function of degree 4 to model hydrostatic effect:

$$f_{hydro}(Z) = a_1 \cdot Z + a_2 \cdot Z^2 + a_3 \cdot Z^3 + a_4 \cdot Z^4 \tag{2}$$

where Z represents the relative trough.

$$Z = \frac{RN - R}{RN - R_0} \tag{3}$$

where RN, R_0, R are respectively the full, minimum and real reservoir water level.

The function f_{ther} depends on temperatures, represented by the sum of four sine functions.

$$f_{ther}(\varphi_S) = a_5 \cdot \cos(\varphi_S) + a_6 \cdot \sin(\varphi_S) + a_7 \cdot \cos(2 \cdot \varphi_S) + a_8 \cdot \sin(2 \cdot \varphi_S) \tag{4}$$

where the season is taken into account using the angle φ_S between 0 radian (1st January) and 2π radians (1st January of the next year).

The function f_{irre} is used to model the time-variant and irreversible response due to the sensors ageing, foundation settlements, soil consolidation and engineering works, etc. (the time unit is the year and the time zero corresponds to the 1st January of the studied period) [16]

$$f_{irre}(t) = a_9 \cdot e^{-\frac{t}{t_0}} + a_{10} \cdot t \tag{5}$$

where t_0 (in year) is a constant of exponential damping time. It can be given by users or determined automatically. It should be noted that some authors used other algebraic forms to model the irreversible term [13]. For the sake of simplicity, a simple linear term is adopted in the following described EFR model which is commonly employed in practice [17]. A further discussion on the different irreversible term versions is provided in the later part of the article.

Although this model has been commonly and successfully used in various dams [18–20], it has some limitations in different aspects:

1. The real temperature is not taken into account for the modelling of thermal effects. A term φ_S representing the season is introduced to approximate this effect,
2. The delayed hydrostatic effect, which is important for some cases of monitoring, is ignored in this model,
3. Rainfalls, which have not been taken into account by the HST model, may influence leakages,
4. The governing variables are supposed to be independent, although it has been shown that some of them are correlated [21].

For the particular case of analyzing pore water pressures in embankment dams, the limitation of using the HST model is that the delayed hydrostatic effect is not taken into account. This model considers that the effect of variations in reservoir water levels on pore water pressure is instantaneous, while it is in fact non-instantaneous and is delayed by the low hydraulic conductivity of materials constituting the embankment. In addition, modelling of the thermal effects, as done in the HST model, is not necessary since the effects are negligible in embankment dams.

2.2. EFR model

The EFR model, that represents an improvement of the HST model, was designed to analyze the pore water pressures (PWP) for homogeneous earth dams considering a constant hydraulic conductivity. The principle of the model is first to create a new series of the reservoir water level, named equivalent reservoir water level (ERWL), accounting for the hydrostatic effect induced by the previous impounding levels. Second, the HST model is applied to pore water pressure data, using this new water level series as variable. Compared to the conventional HST model, the thermal term disappears, since the effect is negligible inside embankment dams. Thus, the EFR model only accounts for two effects: the irreversible trend and the hydrostatic load which is modelled by using the ERWL. In summary, the following expression gives the algebraic formulation of the EFR model:

$$PWP = a_0 + a_1 \cdot t + a_2 \cdot Z_e(T_0) + a_3 \cdot Z_e(T_0)^2 + a_4 \cdot Z_e(T_0)^3 + a_5 \cdot Z_e(T_0)^4 + \epsilon \tag{6}$$

where PWP is the observed time series of pore water pressure, t is the time, $Z_e(T_0)$ is the equivalent relative trough, depending on T_0 which represents the characteristic delayed time of diffusion in the porous media, and ϵ is a residual error in the linear regression. $Z_e(T_0)$ can be determined using Eq. (3) by replacing the real reservoir water level (R) by the equivalent reservoir water level (ERWL). Coefficients a_0, a_1, a_2, a_3, a_4 and a_5 are determined using a multiple linear regression analysis by minimizing the sum of residual squares. As mentioned above, a simple linear term is adopted here for the modelling of the irreversible effect.

2.2.1. Principle of the ERWL

The ERWL is a new series of reservoir water levels accounting for the effects of the previous impounding levels. It is the most important element in the EFR model since a good ERWL can well simulate the delayed hydrostatic effect. The ERWL is computed by making the assumption that the water flow through the porous embankment can be described with the following differential equation. Eq. (7) results from the use of mass conservation and Darcy's law [22]:

$$S\frac{\partial H}{\partial t} = \nabla \cdot (K \cdot \nabla H) + \Omega \tag{7}$$

where H is the hydraulic head distribution which depends on space coordinates (x, y, z), S is the specific storage coefficient (m^{-1}), K is the hydraulic conductivity (m·s^{-1}), Ω describes the sources or sinks (supposed equal to zero in this study) and the vector differential operator $\nabla = \left(\frac{\partial}{\partial x}, \frac{\partial}{\partial y}, \frac{\partial}{\partial z}\right)$.

Assuming that K is constant, the one-dimensional problem can be written as follows:

$$\frac{\partial H}{\partial t} = D\frac{\partial^2 H}{\partial x^2} \tag{8}$$

with the diffusion coefficient $D = K*S^{-1}$. The pore water pressure (i.e. hydraulic head) in dams does not only depend on the instantaneous value of the loading, but on the convolution integral of an impulse response and the loading conditions [23]. The solution of Eq. (8) can be derived and expressed as a convolution form [16]:

$$H(t) = P(t)*R(t) = \int_{t'=-\infty}^{t'=t} R(t') \cdot P(t-t')dt' \tag{9}$$

where $*$ is the convolution product and $P(t)$ is the impulse response function which depends on the boundary condition. Two cases of boundary conditions are usually distinguished for the impulse function: a theoretical finite media and a semi-infinite media. Table 1 summarizes these two cases.

In general, the sensors located in the upstream part of the backfill are recommended to use the semi-infinite media because the end of flow is far away from these sensors. It can then be regarded as a semi-infinite flow model. On the contrary, the sensors located in the middle or in the downstream part of the backfill are close to the end of flow and the use of finite media seems more appropriate in that case. In practice, it is recommended to carry out a study at first to compare the two diffusion models in terms of correlation coefficient in the multiple linear regression.

2.2.2. Numerical methods for computing the ERWL

For a practical application of the model, two numerical calculation methods for the ERWL are introduced: integral calculation and recurrence. The integral calculation can be used for both finite media and semi-finite media, whereas the recurrence can only be used for finite media, because the primitive of the impulse response integral for semi-finite media is unknown.

According to Eq. (9), the ERWL at a given time t_1, can be estimated considering that it represents the sum of all the variations of water levels before time t_1. In practice, the convolution product between the impulse function and loading conditions is written in the period

$[t_1 - m \cdot T_0, t_1]$. A value of 13 for m is sufficient for the precision of calculation [17]:

$$R_e(t_1) = \int_{t'=t_1-m \cdot T_0}^{t'=t_1} R(t') \cdot P(t_1-t')dt' \tag{10}$$

where $R_e(t_1)$ is the ERWL at the given time t_1

The integral in Eq. (10) can be approximated as follows:

$$R_e(t_1) = \frac{\sum_{i=t_1-m \cdot T_0}^{i=t_1-1} P(t_1-i) \cdot R(i) \cdot \Delta t}{\sum_{i=t_1-m \cdot T_0}^{i=t_1-1} P(t_1-i) \cdot \Delta t} \tag{11}$$

Also from Eq. (9), the ERWL at a given time $(t_1 + \Delta t)$ can be expressed:

$$R_e(t_1 + \Delta t) = \int_{-\infty}^{t_1} R(t') \cdot P(t_1 + \Delta t - t')dt' + \int_{t_1}^{t_1+\Delta t} R(t') \cdot P(t_1 + \Delta t - t')dt' \tag{12}$$

Assuming that the $R(t)$ is constant during the calculation interval Δt, Eq. (12) can be written in a recurrence way by calculating the well-known primitive of the impulse response for finite media.

$$R_e(t_1 + \Delta t) = R_e(t_1) \cdot e^{\frac{-\Delta t}{T_0}} + R(t_1 + \Delta t) \cdot \left(1 - e^{\frac{-\Delta t}{T_0}}\right) \tag{13}$$

These two methods (Eqs. (11) and (13)) are applied to a real case study and compared in the second part of the article.

2.2.3. Characteristic delayed time T_0

Another important concept in the EFR model is the characteristic delayed time T_0. It represents the characteristic delayed time of diffusion in porous media. It defines the shape of impulse response (see in Table 1) i.e. weighting function for the computation of the ERWL and can quantify the delay time. The higher the T_0, the longer the time required to reach the final response value (and thus the delay). A very large characteristic time T_0 indicates either that the ground is not saturated (Saturation < 85%), the degree of permeability is very low or the flow distance is very long. When the T_0 is very short (saying close to 0), the response is considered to be instantaneous [23]. For a better understanding, a more explicit parameter T_{90} related to the delay analysis in the EFR model can be introduced. It corresponds to the time taken in the integration of impulse response to reach 90% of the final value. Simon [16] indicated that T_{90} is approximated to $8.5 \times T_0$ for semi-infinite media and $2.3 \times T_0$ for finite media.

Due to the lack of measurements for the dam's physical parameters such as the specific storage coefficient S and the hydraulic conductivity K, T_0 cannot be computed using the equations in Table 1. In order to determine the value of T_0 for each sensor, an optimization procedure is thus proposed. To do this, several values of T_0 are needed to be tested in a physical range, normally form 1 to 200 days [14]. For each T_0, an ERWL is firstly calculated with one of the two methods (Eq. (11) or Eq. (13)) using the reservoir water level measurements of the studied period. Then, a multiple linear regression is conducted for the pore water pressure measurements with the computed ERWL following Eq. (6). The sum of square residues of each regression can be obtained. The optimized value of T_0 corresponds to the minimum of the square residues sum.

2.3. Results of the EFR model analysis

Two major results can be obtained by an EFR model analysis. One is the delayed hydrostatic effect, and another one is the so called 'corrected measurements' (CM).

The delayed hydrostatic effect can be determined by using the following equation derived from Eq. (6).

$$Delayed\ hydrostatic\ effect = a_2 Z_e(T_0) + a_3 Z_e(T_0)^2 + a_4 Z_e(T_0)^3 + a_5 Z_e(T_0)^4 \tag{14}$$

Table 1
Solution and characteristics of the diffusion equation.

$$P(t) = \frac{1}{T_0} \cdot e^{\frac{-t}{T_0}} \text{ with } T_0 = \frac{L^2 \cdot S}{K \pi^2}$$

(a) Finite media

$$P(t) = \sqrt{\frac{T_0}{\pi}} \cdot \frac{e^{\frac{-T_0}{t}}}{t^{1.5}} \text{ with } T_0 = \frac{x^2 \cdot S}{4 \cdot K}$$

(b) Semi-infinite media
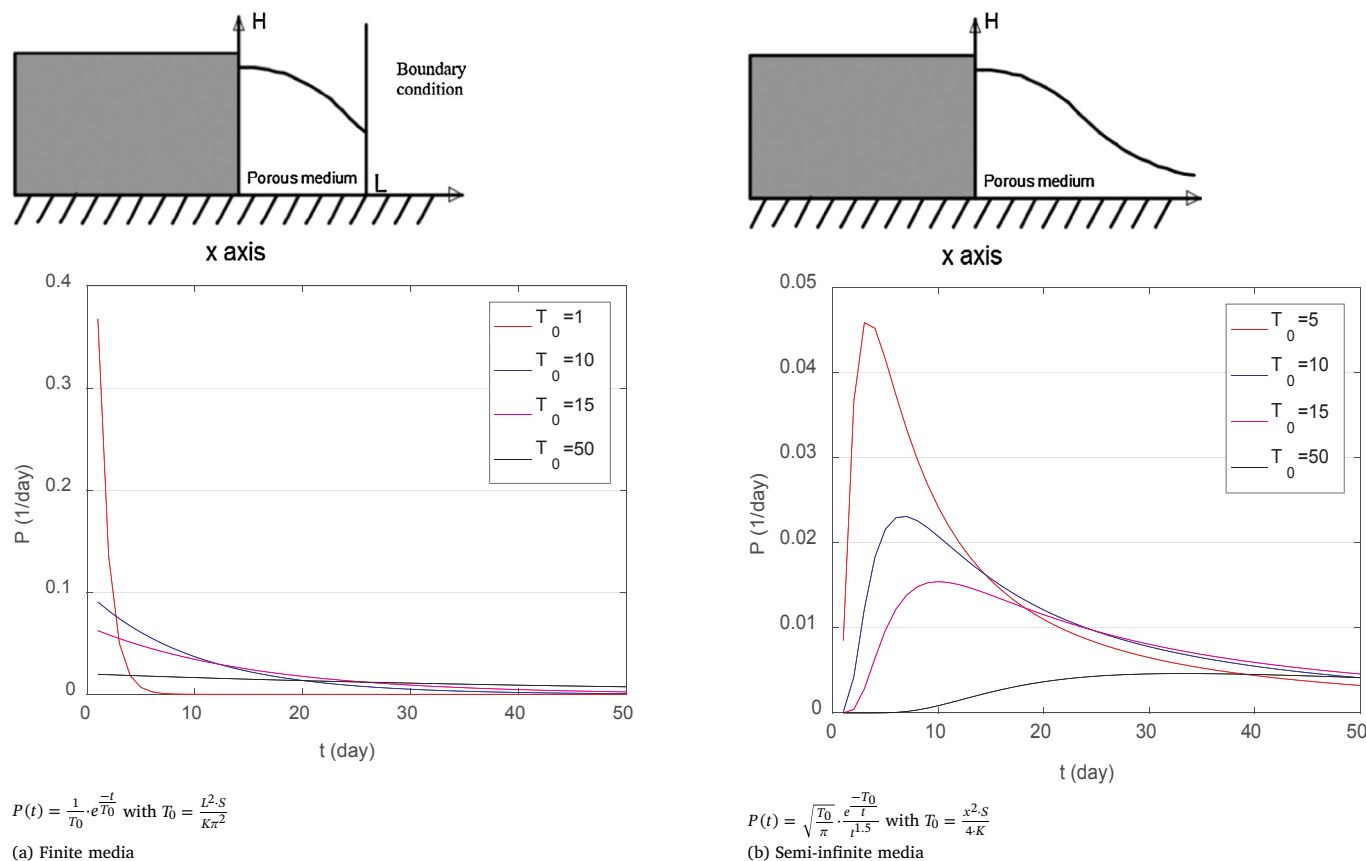
Where x is the distance traveled by the water between the reservoir and the sensor (m), S the specific storage coefficient (m^{-1}), K the hydraulic conductivity (m·s^{-1}) and L the length of the finite media in which diffusion occurs (m).

It represents the component of PWP induced by the difference between the ERWL and reference water level (full reservoir water level in the case). It is reminded here that $Z_e(T_0)$ is the equivalent relative trough and can be calculated using Eq. (3) by replacing the real reservoir water level (R) by the equivalent reservoir water level (R_e). By deducting this component from the raw measurements (RM) of PWP, the CM is obtained:

$$CM = PWP - a_2 \cdot Z_e(T_0) - a_3 \cdot Z_e(T_0)^2 - a_4 \cdot Z_e(T_0)^3 - a_5 \cdot Z_e(T_0)^4 \quad (15)$$

One can also express CM as following according to Eq. (6):

$$CM = a_0 + a_1 \cdot t + \epsilon \quad (16)$$

CM represents the measurements of PWP in identical hydrostatic loading conditions over time. According to Eq. (15), it is obtained by deducting the delayed hydrostatic effect with respect to the reference water level from the raw measurements (PWP). If the effect is perfectly simulated, it will be completely eliminated form PWP, and CM contains only a constant average, irreversible effects and a regression error. By ensuring a good performance of the regression (small value of ϵ), the evolution of the irreversible effect under constant loads can then be quantified and highlighted by the CM. A good estimation of irreversible trend of PWP enables us to understand better the evolution response of dam over time and to detect early the abnormal events. The irreversibility of PWP can be associated with ageing of sensors, settlement of foundation, consolidation and creep of backfill and unusual loads (earthquake, hydrostatic load outside the normal operations, engineering works, etc.).

The obtained CM can be compared to the specific raw measurements, in order to modify its absolute value and thus improve its

physical meaning. The raw measurements used for such comparison are those collected when the reservoir water level is maintained full for a period longer than T_{90} (2.3T_0 for the finite diffusion model and 8.5T_0 for the semi-infinite diffusion model) [16]. Regarding the sensors far away from the hydrostatic load, this period can be very long, typically in the order of several months. Most of the time, the water level is not kept full for several months. For this reason, it is recommended to carry out this comparison at a lower level such as the average or minimum equivalent water level, since it is possible to find a period of maintaining such water levels longer than T_{90}. To predict the pore water pressure (CM_d) at a desired water level using the EFR model, one can firstly conduct an EFR analysis, following the procedure described in the next section, to obtain the corrected pore water pressure at the full reservoir water level noted as CM_{full}. The CM_d is then computed by adding the corresponding delayed hydrostatic effect of the desired water level, determined by Eq. (14), to the CM_{full}. Thereafter, the obtained CM_d is compared with the PWP measurements when the reservoir water level is maintained at the desired level for a period longer than T_{90}.

It should be emphasized that this comparison is not a compulsory step for an EFR analysis, since it does not calculate the delayed characteristic time and the irreversible evolution of the measurements. Performing this comparison for the EFR model is just a way to have a general idea about the absolute value of the obtained CM_d and to improve its physical meaning.

2.4. Procedure of the EFR model

For practical applications, a general description on how to use the EFR model is provided:

1. Determination of the studied period, the full and minimum reservoir water levels,
2. Collection of the raw measurements (reservoir water levels and pore water pressures) in the studied period,
3. Optimization of the characteristic delayed time T_0 for the studied data following the procedure presented in Section 2.2. This term together with T_{90} can give an insight on the delay time,
4. Calculation of the ERWL using one of the two numerical methods presented in Section 2.2 (Eq. (11) or Eq. (13)) with the optimized T_0,
5. Determination of the unknown coefficients in Eq. (6) using a multiple linear regression with the equivalent relative trough Z_e determined by the computed ERWL,
6. Output of the results
   a. Calculation of the CM using Eq. (15) or Eq. (16).
   b. Calculation of the delayed hydrostatic effect using Eq. (14).

Concerning the choice of the diffusion model, Section 3.2 provides a discussion and some recommendations.

3. Application to the reference case: a French embankment dam

This section presents an application of the EFR model on a French embankment dam. The main characteristics of the dam including geometry, monitoring device and experimental data are presented at first. The procedure of using the model to analyze PWP measurements is then presented.

3.1. Geometry, monitoring device and experimental data

Fig. 1 presents the main central cross section of the studied dam. It is a 1 km long and 37 m high homogeneous dam with an upstream impervious face made of concrete. The dam was completed in the 1950s. The first water filling was in 1959. After that, there were several repairs and rehabilitation works for the concrete slab of the upstream, the drainage system and the berms in downstream. The piezometric sensors started to be installed in the dam since 1987 and completed in the year 1990.

The foundation is made up of sandy and gravely alluvium due to granite erosion, granitic area and fissured granite, in which a grout curtain of bentonite-cement and silicate aluminate was realized with a depth of around 20 m. Concerning the drainage system, a layer about 50 cm depth constituted with gravels is located in the upstream below a concrete slab and some drains prolonged by a rock-filled mass are placed at the downstream foot.

The dam itself is mainly constituted of gravel moraine collected from a terrace located 500 m from the downstream. Fig. 2 presents the maximum and minimum passing percent of a grain size analysis for different soil samples in the backfill. The mean curve gives about 45%
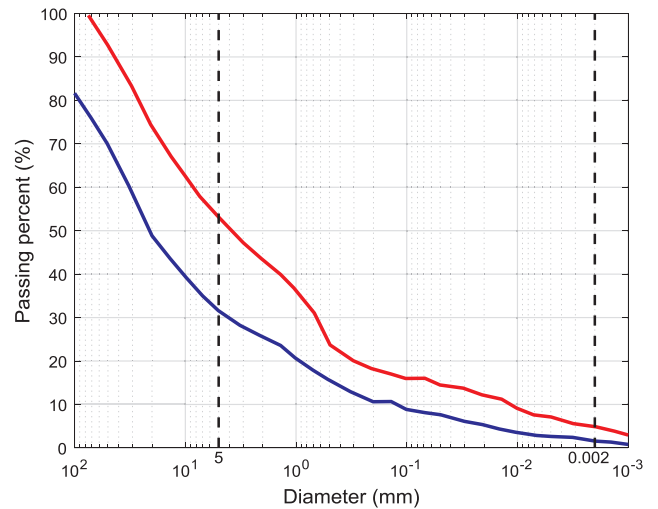
Fig. 2. Maximum and minimum passing percent of the grain size distribution for the material constituting the backfill (derived from the construction report of the dam).

of elements smaller than 5 mm and just 4% of clay (grain size smaller than 2 μm). The hydraulic conductivity at saturation of such material is assumed to vary from 10^{-4} to 3×10^{-5} m/s, according to the predictive models resumed in [24]. After compaction, the dry density is 2.15 and the water content is about 7%.

The main central cross section (section A-A in Fig. 3), as show in Fig. 1, is instrumented with 5 piezometric sensors, denoted PP1 to PP5. Respectively in the location of these five sensors, five other piezometric sensors, denoted PP6 to PP10, are identified in another cross section (section B-B in Fig. 3), which has approximately the same geometry as the main central cross section. These two sections are studied using the EFR model in the paper. The setting up of these sensors is presented in Fig. 3 from a top view of the studied dam.

A pore water pressure sensor is composed of vibrating wire piezometers embedded within the embankment. Measurements obtained by these sensors were gathered from the first impoundment. For the whole dam, there are mainly five types of monitoring devices for different surveillance purposes. Table 2 summarizes all the devices used in this dam.

Two types of data are analyzed in the study: one is reservoir water levels of the dam which is measured with a daily time step from the 31/03/1960 to the 18/03/2015, another is the PWP levels inside the dam measured every 15 days since the year 1990. Fig. 4 plots the time series of water levels and PWP levels of the sensors PP1 to PP5 for the year 2014.

First, it can be observed from Fig. 4 that the evolution of water levels was nearly seasonal for year 2014 with low levels in March-April
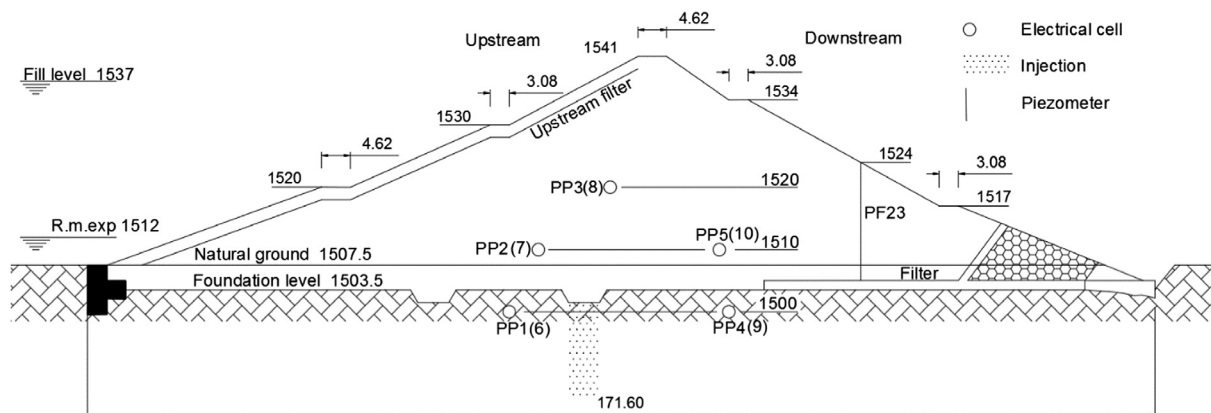
Fig. 1. Main central cross-section of the studied embankment dam and location of the vibrating wire piezometers (PP1 to PP5).
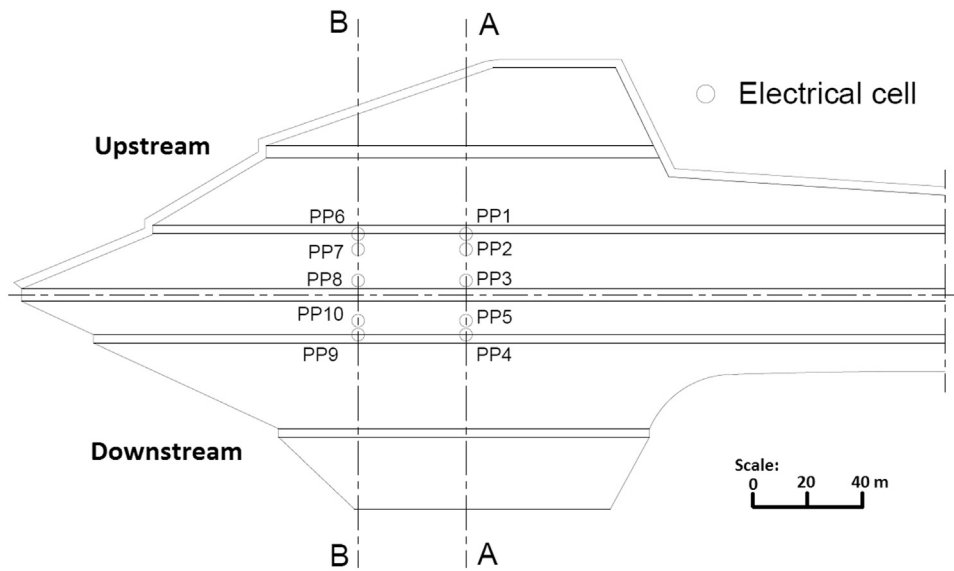
Table 2
Information relative to the monitoring devices used in the studied dam.

Type of sensors	Quantity	Location	Remark
Planimetrics	4	Crest	Topographic survey
	7	Top berm of downstream	
	3	Below berm of downstream	
	1	Foot of the dam	
Levelling	8	Crest	Crest settlement marks
	7	Top berm of downstream	
	3	Below berm of downstream	
Electrical cells	5	Section A-A	Piezometric level
	5	Section B-B	
Piezometers	8	Shoulder of left bank	Piezometers
	4	Downstream filter	
Leakage	17	The whole dam	Seepage measurements
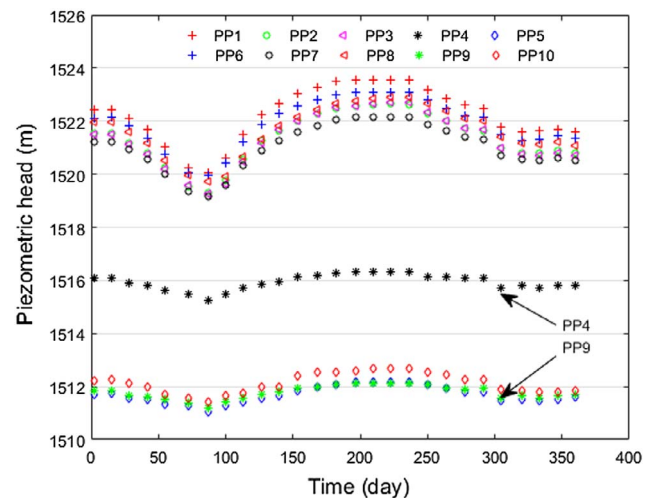
Fig. 5. Comparison of the raw measurements for the ten sensors (year 2014).
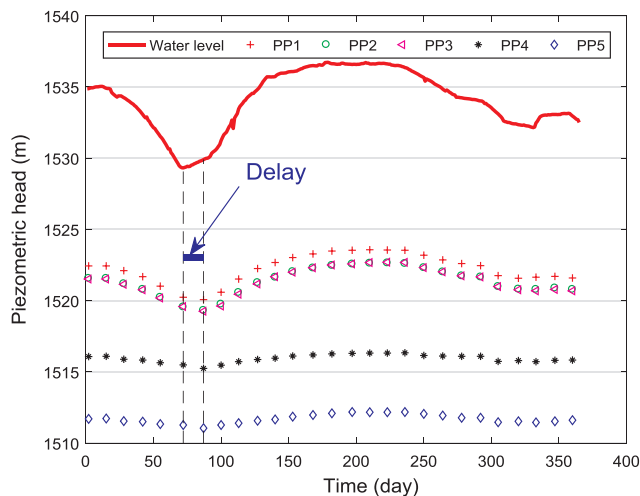
Fig. 4. Evolution of reservoir water levels and piezometric levels for the sensors PP1 to PP5 (year 2014).

and high levels in June-July-August. Then, a decrease of the piezometric levels from upstream (PP1) to downstream (PP4) is identified. In addition, the minimum in the reservoir water level does not occur at the

same time for these five sensors. In fact, there is a time delay between the reservoir water level and piezometric level which is due to the fact that water seepage in porous media is not instantaneous. Therefore, it seems compulsory to use a model which is able to account for the delayed effect. An abnormal phenomenon is inferred from Fig. 4. Particularly, the piezometric level for the sensor PP4 is always higher than that of the sensor PP5, although PP4 is farther to the hydrostatic load than the PP5. Following this observation, a comparison of the piezometric level evolution between the sections A-A and B-B is carried out in order to analyze the raw measurements for these ten sensors. These sensors can be divided into five couples: PP1-PP6, PP2-PP7, PP3-PP8, PP5-PP10 and PP4-PP9. In each couple, the piezometric level evolutions of sensors should be approximately equal to the other because they are located at the same position in the X-Y plan (see in Fig. 1), respectively in the section A-A and B-B. It is well confirmed by the first four couples, whereas the piezometric levels evolution for the sensor PP4 is always much higher than the one of the sensor PP9 (see in Fig. 5). Considering this comparison study and the abnormal phenomenon observed in Fig. 4, there is probably a local effect in the section A-A for the sensor PP4.

Table 3
Comparison of the correlation coefficients for the diffusion models and the numerical methods of ERWL computation.

Sensor	Semi-infinite media	Finite media	
	Integral calculation	Integral calculation	Recurrence
PP6	0.9873	0.9874	0.9878
PP7	0.9716	0.9717	0.9745
PP8	0.9547	0.9573	0.9649
PP10	0.9197	0.9299	0.9351
PP9	0.9411	0.9440	0.9512

3.2. Diffusion models and numerical calculation methods of ERWL

A preliminary study aims at comparing the two diffusion models (Table 1) in order to choose the best approach for the case study. A criterion used to realize these comparisons is the correlation coefficient between the raw measurements PWP and the endogenous variable of the multiple linear regression ($PWP - \epsilon$) (see in Eq. (6)). The closer this coefficient is to 1, the stronger the linear relation between the two variables is. It can be calculated by conducting the steps 1 to 5 of the procedure described in Section 2.4.

Table 3 summarizes the correlation coefficients for the two diffusion models, knowing that for the finite media model, the ERWL is calculated using the two computation methods presented previously. This study is carried out for the sensors of the section B-B with totally 327 measurements from the year 2003 to 2015. It should be mentioned that the characteristic delayed time T_0 is not the same for different diffusion models and different numerical methods, and should be determined by an optimization procedure at first.

As can be seen from Table 3, all correlation coefficients are higher than 0.91 even 0.98 for the sensor PP6. Both the finite and semi-finite diffusion model can perform a good multiple linear regression by generating an adapted series of ERWL. For the studied dam, it seems that the finite media is more appropriate because the presence of downstream filter induces a distribution of PWP quite similar to the finite media. Regarding the numerical method for calculating the ERWL, the recurrence calculation performances are better than the integral calculation. Indeed, the integral calculation is realized with the rectangle method, which is an approximation of 0 order, whereas the primitive function can be derived and used for the recurrence calculation, which is hence more accurate. Consequently, a finite media with recurrence calculation is selected as the optimized model for the following study.

3.3. Optimized values of T_0

Following the procedure presented in Section 2.2, the optimized value of characteristic delayed time T_0 is obtained. Table 4 summarizes the obtained T_0 for the ten sensors. The study period is always from the year 2003 to 2015 as mentioned in Section 3.2.

As presented in Table 4, the variation range of characteristic delayed time T_0 for the ten sensors is from 4.7 to 13.8 days with an average

Table 4
Characteristic delayed time T_0 of the sensors from PP1 to PP10.

	T_0 (day)		Absolute difference (day)
	Section AA	Section BB	
PP1(6)	4.7	5.1	0.4
PP2(7)	6.8	7.1	0.3
PP3(8)	7.9	7.9	0
PP5(10)	13.8	13.4	0.4
PP4(9)	10.9	7.8	3.1

value of 8.6 days. The sensors located in the same position of different sections, as expected, have almost the same value of T_0 since their absolute differences are all smaller than 0.4 days, except the sensor PP4(9). This inconsistency can be explained by the fact that there is a local effect for the sensor PP4 as analyzed in Section 3.1. Besides, the characteristic time T_0 depends on the position of the measuring instrument with respect to the upstream hydrostatic load. Theoretically, sensors that are far away from the hydrostatic load have a higher T_0 than sensors close to the water level. This is the case for the sensors presented in Table 4 except the sensor PP4(9). These two sensors are located near to and lower than the downstream filter which can drawdown the PWP level and reduce the diffusion time (as presented in Fig. 1).

3.4. EFR model analysis results

Once the diffusion model, numerical calculation method for ERWL and optimized value of T_0 are determined, an EFR model analysis can be conducted. The CM and delayed hydrostatic effect are obtained by performing the steps 4–6 of the procedure. In this section, the finite diffusion model and the recurrence calculation method are adopted.

Fig. 6 shows that the ERWL has the same shape as the curve of real reservoir water levels, but this time being almost "in phase" with the curve of piezometric level measured by the sensor PP3. This means that there is nearly no time delay between the ERWL and the sensors piezometric level.

Fig. 7 presents the raw measurements (RM) and corrected measurements (CM) evolution of PP1 for a period of 12 years from 2003 to 2015. The CMs are obtained using Eq. (15) by performing an EFR analysis based on the ERWL. It represents the PWP under the hydrostatic load of full reservoir water level over time. One can observe that the dispersion of the measurements is strongly reduced from RM to CM. The standard deviation decreased from 1.75 m (RM) to 0.36 m (CM) corresponding to a reduction of 82.5% for the measurements coefficient of variation. As the CM correspond to the piezometric levels under the hydrostatic load condition of full water level, it is logical to find that the CMs are always higher than the RMs. Besides, a temporal effect, which describes a slight decrease of measurements with time evolution especially after the date '18/11/2010', can be observed in the CM thanks to its limited dispersion. This observation can help to track any abnormalities. The significant decrease of CM after 2010 may be related to the engineering works which occurred in the year 2009 and 2010, when a renovation work for the drainage system in downstream can be found.

Once the linear regression is performed, the delayed hydrostatic effect can be calculated by Eq. (14). As illustrated in Fig. 8, it is simply
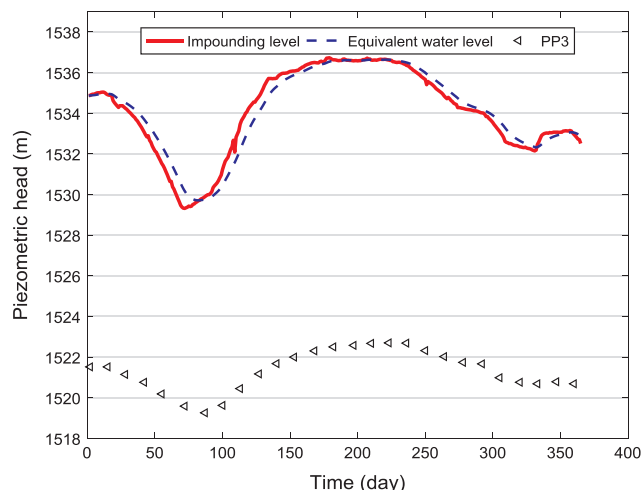
Fig. 6. Illustration of the ERWL calculated by EFR model (finite media, recurrence method, $T_0 = 7.9$ days) for the year 2014.
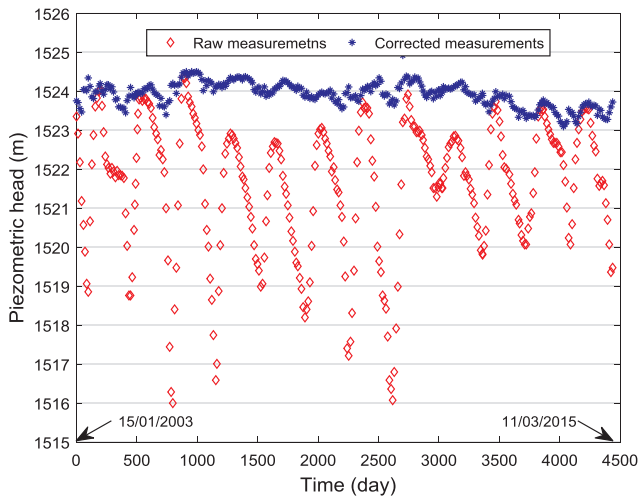
Fig. 7. Corrected measurements for the sensor PP1 using the EFR model (finite media, recurrence method, $T_0 = 4.7$ days).
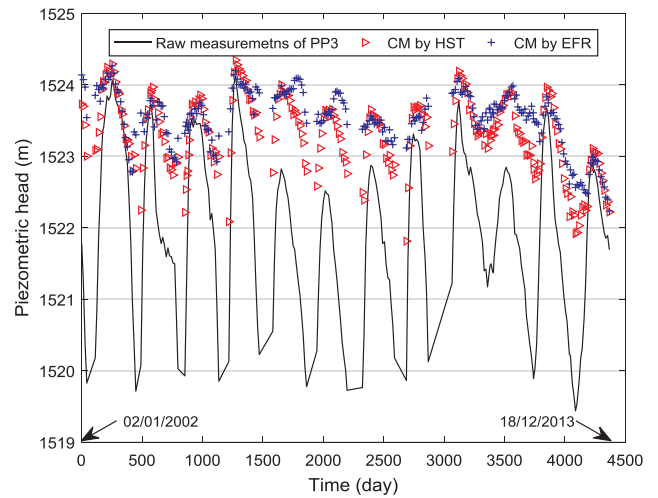
Fig. 9. Comparison of corrected measurements for sensor PP3 between HST and EFR models.

lead to better results of CM than using directly the reservoir water level measurements.
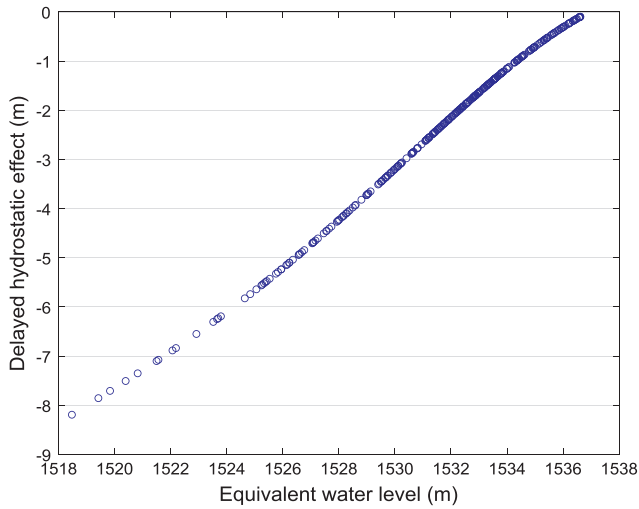
Fig. 8. Delayed hydrostatic effect for sensor PP1 using the EFR model.

the polynomial of ERWL and it ranges from -8.2 to -0.1 m. It is worth noting that the ERWL is obtained by maintaining a constant water level during a delay that is greater than the characteristic time T_{90}: approximately $2.3.T_0$ for finite media and $8.5. T_0$ for semi-infinite media [16].

3.5. Further discussion

3.5.1. Comparison between the HST and EFR models

Fig. 9 illustrates the comparison between the raw measurements and corrected measurements of the sensor PP3, respectively obtained by HST and EFR models for the years from 2002 to 2013. The used HST model for the comparison is described in Section 2.1 with neglecting the thermal term f_{ther}. The EFR model analysis is conducted by following the procedure described in Section 2.4. As mentioned in Section 2.3, the hydrostatic loading effects with respect to the reference water level should be completely eliminated from the RM if they are perfectly simulated. The term CM will only contain a constant average, the irreversible effects and a regression error. It can be observed from Fig. 9 that there is still a visible seasonal aspect in the CM by HST, which is more reduced with the EFR model. In addition, the dispersion of the CM by EFR is strongly reduced. The observations confirm that the modelling of hydrostatic effects in EFR model is better done than in the HST model. Using the ERWL in which the delayed effect is considered, will

3.5.2. Different versions of irreversible term

As mentioned above, some authors used different algebraic forms to model the irreversible effect. Five versions of irreversible term can be identified according to [13]. A comparison study is carried out in this section to study the influence of the irreversible term version on the CM. The study is based on the sensor PP1 with a totally 327 measurements from the year 2003 to 2015. The five versions of irreversible term are:

1. Mata [25]: $a_1 t + a_2 e^{-t}$
2. Chouinard [26]: $a_1 t$
3. Original form [5]: $a_1 \log(t) + a_2 e^t$
4. Simon [27]: $a_1 e^{-t/t_0} + a_2 t + a_3 t^2 + a_4 t^3 + a_5 t^4$
5. Yu [28]: $a_1 t + a_2 t^2 + a_3 t^3$

Five EFR analyses are conducted following the procedure described in Section 2.4, using respectively the five irreversible term versions to simulate the irreversible effects. Five series of CMs are thus obtained by these five analyses and are presented in Fig. 10. In addition, the correlation coefficient, the statistic moments of CM and the characteristic delayed time T_0 for the five versions of irreversible term are compared
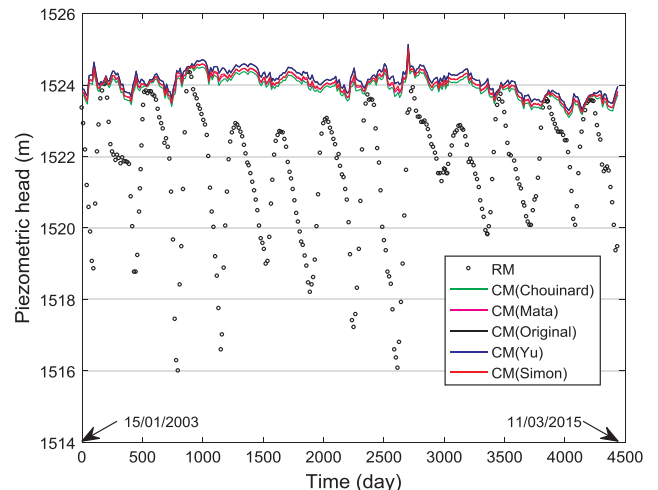
Fig. 10. Comparison of the CM of sensor PP1 for five versions of irreversible term.

Table 5
Partial EFR model results for the five versions of irreversible term (sensor PP1).

Version	Correlation coefficient	Mean value of CM (m)	Standard deviation of CM (m)	Characteristic delayed time T_0 (day)
Chouinard	0.989	1523.92	0.307	4.7
Mata	0.991	1524.01	0.311	5.0
Original	0.990	1524.00	0.309	4.9
Yu	0.993	1524.13	0.317	5.0
Simon	0.993	1524.15	0.317	5.1

in Table 5. Particularly, the optimized value of parameter t_0 (in year) in the model of Simon [27] should be firstly determined by assuming a constant T_0. It represents the characteristic time of exponential damping for the irreversible effect. Then, the EFR model is conducted using this optimized t_0. The optimization criterion is always the correlation coefficient between the raw measurements PWP and the endogenous variable of the multiple linear regression (PWP-ε) (see in Eq. (6)).

One can observe from Fig. 10 that the CMs obtained with the five versions of irreversible term have the same evolution form, so reflect the same irreversible trend. The values of the five CMs are in good agreement with each other. From Table 5, it can be concluded that all the five versions of irreversible term have a good performance in the linear regression since the correlation coefficients are all extremely close to 1. In addition, the difference of the mean and standard deviation of CM among the five versions is negligible. And they give similar values for the characteristic delayed time T_0, which is between 4.7 and 5.1 days. Based on Fig. 10 and Table 5, it seems that there is no influence of the irreversible term version on the CM and it is sufficient to use a linear term to model the irreversible effect on pore water pressure inside embankment dams. This finding can be extrapolated to the application of the EFR model for any embankment dams. An interpretation is as follows. By using the CM to illustrate the irreversible trend, it is not necessary to assume any hypothesis regarding the algebraic expression of the irreversible effect. The key problems are to guarantee a good modelling of the hydrostatic effect and a good performance of the multiple linear regression. Using an exponential, logarithmic or linear term to simulate the irreversible effect is just a way to calibrate the linear regression. The obtained hydrostatic effect and CM are changeless regarding to the form of the irreversible term (confirmed by Fig. 10 and Table 5). Thus, the version of the irreversible term has almost no influence on the EFR analysis results. In addition, the linear time effect used to calibrate the multiple linear regression is less important regarding the irreversible trend of CM, and can be easily calibrated on a time-linear behaviour of PWP [14]. For the sake of simplicity, it is recommended to use the simple linear term to model the irreversible effect of PWP.

4. Conclusion

The paper presents an analytical model named EFR (EFfet Retard - Delayed effect) for the prediction of pore water pressure inside embankment dams. This model is able to take into account delayed effects between the changes of reservoir water level and the monitoring device located inside homogeneous dams, due to the hydraulic diffusivity. Applying the model to dam monitoring data permits to obtain the corrected measurements which represent measurements under identical loading conditions over time. These corrected measurements can therefore highlight and quantify the irreversible evolution trends occurring under constant loads. A good estimation of irreversible effect enables us to understand better the evolution response of dam over time and to detect early the abnormal events. At the same time, the delayed hydrostatic effect can be isolated and quantified.

An application of the model to a French embankment dam is provided in the paper. The corrected measurements of pore water pressure

are obtained using the equivalent reservoir water level computed with the optimized characteristic time T_0. The dispersion of raw measurements has been strongly reduced by applying this model. Particularly, the diffusion models, the numerical methods of computing the equivalent reservoir water level and the different versions of irreversible term are discussed. The results show that both the diffusion models and the numerical methods can perform a good linear regression for the study case, and a linear term is sufficient to model the irreversible effect. Besides, a comparison between the HST and EFR models is carried out and confirmed the good performance of the EFR model.

As presented in this paper, the results obtained by EFR model permits a better restitution of the observed evolution. In order to continually improve the performances of EFR model. ongoing works will consist in taking into account the downstream water level and the rainfalls [29].

Symbol list

Some important symbols and abbreviation used in the article are listed in the following table.

Important symbols

a_0	Average value in the multiple linear regression
t (year)	Time
ϵ	Residual error in the linear regression
R	Real reservoir water level
R_e	Equivalent reservoir water level
Z_e	Equivalent relative trough $\left(Z_e = \frac{RN - R_e}{RN - R_0} \right)$
T_0 (day)	Characteristic delayed time
T_{90} (day)	The time taken in integration of impulse response to reach 90% of the final value
P (1/day)	Impulse response
S (m^{-1})	Specific storage coefficient
K (m·s^{-1})	Hydraulic conductivity
L (m)	The length of the finite media in which diffusion occurs.
x (m)	The distance traveled by the water between the reservoir and the sensor (m)

Abbreviation

HST	Hydrostatic-Season-Time
EFR	EFfet-Retard (French), delayed effect
RM	Raw Measurements
CM	Corrected Measurements
ERWL	Equivalent Reservoir Water Level
PWP	Pore Water Pressure

References

[1] Johansson S. Seepage monitoring in embankment dams; 1997.
[2] Santillan D, Fraile-Ardanuy J, Toledo MA. Dam seepage analysis based on artificial neural networks: The hysteresis phenomenon. In: Proc. int. Jt. conf. neural networks; 2013.
[3] Crepon O, Lino M. An analytical approach to monitoring. Int Water Power Dam Constr 1999;51(6):52–4.
[4] Ferry S, Willm G. Méthodes d'analyse et de surveillance des déplacements observés par le moyen de pendules dans les barrages. In: VIth international congress on large dams; 1958. p. 1179–201.

[5] Willm G, Beaujoint N. Les méthodes de surveillance des barrages au service de la production hydraulique d'Èlectricité De France. In: IXth international congress on large dams; 1967. p. 529–50.

[6] Penot I, Daumas B, Fabre J-P. Monitoring behaviour. Int Water Power Dam Constr 2005;57(12):24–7.

[7] Wu K, Ma M, Hao D, Chen R. Numerical analysis on mechanics of interaction between slurry and soil in earth dam by splitting grouted. Proc Eng 2012;28(2011):351–5.

[8] Pan Q, Dias D. The effect of pore water pressure on tunnel face stability. Int J Numer Anal Methods Geomech 2016;40(15):2123–36.

[9] Pan Q, Xu J, Dias D. Three-dimensional stability of a slope subjected to seepage forces. Int J Geomech 2017(March):4017035.

[10] Pagano L. Pore water pressure measurements in the interpretation of the hydraulic behaviour of two earth dams, no. January 2015; 2010.

[11] Bonelli S, Royet P. Delayed response analysis of dam monitoring data. In: ICOLD European symposium on dams in a European context; 2001.

[12] Lombardi G, Amberg F, Darbre GR. Algorithm for the prediction of functional delays in the behaviour of concrete dams. Int J Hydropower Dams 2008;15(3):111–6.

[13] Salazar F, Morán R, Toledo M, Oñate E. Data-based models for the prediction of dam behaviour: a review and some methodological considerations. Arch Comput Methods Eng 2015;24(1).

[14] Simon A, Guilloteau1 T. Analysis method for the monitoring of pore water pressure in embankment dams. In: 84th ICOLD annual meeting; 2016.

[15] Chouinard L, Roy V. Performance of statistical models for dam, vol. 2211; 2006. p. 199–207.

[16] Simon A. Analyse des effets retards description et application de la méthode EFR utilisée lors du dépouillement des mesures; 2014.

[17] Simon A, Royer M, Mauris F, Fabre J-P. Analyse des mesures d ' auscultation des barrages avec les réseaux de neurones Analysis and Interpretation of Dam Measurements using Artificial Neural Networks. Colloq. CFBR; 2012. p. 1–15.

[18] Dibiagio E. Monitoring of dams and their foundations. In: XXth international congress on large dams; 2000. p. 1459–545.

[19] Guedes Q, Coelho P. Statistical behaviour model of dams. In: XVth international congress on large dams; 1985. p. 319–34.

[20] Chouinard L, Roy V. Performance of statistical models for analyzing the long term behaviour of dams. In: 2nd conference on long term behaviour of dams; 2009. p. 141–6.

[21] Salazar F, Toledo MA, Oñate E, Morán R. An empirical comparison of machine learning techniques for dam behaviour modelling. Struct Saf 2015;56:9–17.

[22] Bear J. Dynamics of fluids in porous. Media 2013.

[23] Bonelli S, Royet P. Delayed response analysis of dam monitoring data; 2001.

[24] Chapuis RP. Predicting the saturated hydraulic conductivity of soils: a review. Bull Eng Geol Environ 2012;71(3):401–34.

[25] Mata J, Tavares de Castro A, Sá da Costa J. Time-frequency analysis for concrete dam safety control: correlation between the daily variation of structural response and air temperature. Eng Struct 2013;48:658–65.

[26] Chouinard L, Roy V. Performance of statistical models for dam. Jt Int Conf Comput Decis Mak Civ Build Eng 2006;2211(August):199–207.

[27] Simon A, Royer M, Mauris F, Fabre J. Analysis and interpretation of dam measurements using artificial neural net works. In: 9th ICOLD European club symposium; 2013.

[28] Yu H, Wu ZR, Bao TF, Zhang L. Multivariate analysis in dam monitoring data with PCA. Sci China Technol Sci 2010;53(4):1088–97.

[29] Bonelli S. Approximate solution to the diffusion equation and its application to seepage-related problems. Appl Math Model 2009;33(1):110–26.